DELIVERY OF A FATTY ACID SIGNAL VIA RTIL FOR BIOFILM DISPERSION

by
Rachaud Keyes

A thesis submitted to the faculty of The University of Mississippi in partial fulfillment of the requirements of the Sally McDonnell Barksdale Honors College.

Oxford
May 2015

Approved by

_____
Advisor: Dr. Paul Scovazzo

_____
Reader: Dr. John O'Haver

_____
Reader: Dr. Adam Smith

ACKNOWLEDGEMENTS

At this point, I wish to express my sincerest thanks to my research advisor, Dr. Paul Scovazzo, and my two remaining readers for this thesis, Dr. John O'Haver and Dr. Adam Smith – for they have shared their expertise in their respective fields in guiding my thesis. I also would like to thank the Sally McDonnell-Barksdale Honors College for the research opportunity and appropriate funding for developing the laboratory research associated with this thesis.

ABSTRACT

A number of proposed applications for ionic liquids involve ionic liquid/water interfaces, such as, chemical separations or drug delivery systems. Therefore, an understanding of the solubility and micellar behavior of ionic liquids in an aqueous environment is critical fundamental knowledge. The long term goal of our study was ionic liquids for delivery of biological active agents; therefore, we chose the anion, bis(trifluoromethanesulfonyl)imide (Tf_2N) since it promotes water stability and forms water immiscible RTILs. The study then paired the Tf_2N-anion with three different classes of cations. By adding apolar substituents ($-CH_2-$) to the cation, the size of the molecule increases in each RTIL class, rendering the RTIL less soluble in the water phase. The three classes of RTILs examined were 1-Cn-3-methylimidazolum (Rmim), Cn-trimethylammonium (CTA), and branched ammonium (BAM), with the "Cn" representing an alkyl functional group (propyl, butyl, etc.). For industrial use, CTAs are attractive, since they can be synthesized from inexpensive ammonium surfactants. However, large CTAs (twelve carbon chain and higher) are solids at ambient conditions. In contrast, BAMs have larger compounds that remain in the liquid state at ambient conditions. Nevertheless, each class has potential as a delivery agent by meeting the aforementioned criterion – namely, water immiscible and water stable at ambient temperatures. We used Total Organic Carbon (TOC) analysis to determine the RTIL content in water that is in equilibrium with the tested RTILs. Surface tension measurements of the RTIL containing water determined if RTIL micelles existed in the RTIL saturated water. We used LFER (Linear Free Energy Relationship) semi-empirical models to correlate the RTIL water solubility to the molecular size and structure of the

RTIL cation. Combining the LFER results with surface tension measurements and thermodynamic calculations of sub-cooled RTIL fugacities, allowed us to determine that micelle formation is not significant for the tested RTILs with molar volumes less than 350 cm^3/mol. We tested a total of 15 different RTILs with the water solubilities ranging from 10^{-2} to 10^{-4} moles-RTIL/L-water. Based on the water solubilities, the proposed RTILs are [N(10)111][Tf_2N], [N(10)Me_2(iPr)][Tf_2N], and [C(6)MIM][Tf_2N] for delivery of the signal cis-2-decenoic acid for biofilm dispersion.

TABLE OF CONTENTS

INTRODUCTION

Biofilm formation (biofouling) is a significant problem affecting a number of industrial applications, such as pipes, heat exchangers, and membranes. Considering many membranes are in contact with water or moist air, living microbes readily form layered colonies or biofilms; as an example of problems associated with biofilms, cleaning of biofilms in reverse osmosis units is a significant operation cost for desalination plants, and biofouling is a major factor leading to the sick-building syndrome. In forming biofilms, bacteria use a number of attachment mechanisms, including flagellar attachment, adhesive proteins, and extracellular polysaccharides in adhering and growing on a surface [1]. To date, researchers have found no surfaces that completely resist biofilm formation; thus, biofilm prevention is nearly impossible [1].

Previous research into biofilm formation found that biofilm formation inversely relates to the polarity of the surface of a membrane [2]. RTIL-membranes present an ionic liquid surface to the contacting fluid. The potential exists that room-temperature ionic liquids will reduce biofilm formation since their surfaces are highly polar, liquid (not a stable foundation for microbe attachment), and salts.

This thesis will provide a basis for management – not eradication – of biofilms from a surface via a fatty acid signal, cis-2-decenoic acid, known to disperse biofilms. To deliver this signal, we propose selecting an RTIL with extremely low solubility in water and high carrying capacity (high solubility of signal in the RTIL) to ensure appropriate in situ delivery via mass transport (RTIL to biofilm).

RTILs are organic salts that remain in the liquid state at ambient temperatures. The asymmetry of the cation is responsible for low lattice energies and the resulting liquid state [3]. In selecting an appropriate RTIL, we only consider water-stable RTILs considering their application in humid environments [4]. The anion, bis(trifluoromethanesulfonyl)imide (Tf_2N), promotes water stability and forms water immiscible RTILs. To determine an optimal RTIL, we chose Tf_2N as the anion for all RTILs; therefore, the focus is on RTIL class (cation) and size.

By adding apolar substituents (-CH_2-) to the cation, the size of the molecule increases in each RTIL class, rendering the RTIL less soluble in the water phase. An empirical model can relate the amount of RTIL partitioned into the water phase at saturation as a function of the size of the molecule. The form of the LFER (Linear Free Energy Relationship) empirical model is $logC_{iw}^{sat}(L) = -a(V_{ix}) + b,$ where $C_{iw}^{sat}(L)$ is the saturation concentration of chemical i in its liquid form in the water phase and V_{ix} is the molar volume of chemical i calculated by a group contribution method, accounting for the intrinsic molecular volume and bulk structure [5].

The three classes of RTIL examined in our study were 1-C_n-3-methylimidazolum (Rmim), C_n-trimethylammonium (CTA), and branched ammonium (BAM) – C_n represents an alkyl functional group (propyl, butyl, etc.). For Rmims, the "C_n" represents the first letter of the alkyl functional group (butyl, hexyl, etc.); Bmim is 1-**b**utyl-3-**m**ethyl**i**midazoliu**m**. For CTAs and BAM, we represent the cation by substituents attached the central nitrogen; for example, [N(4)111] and [BuMe(3)] represent the same butyl-trimethylammonium cation. Each class has an advantage in advancing our study. Literature data ($C_{iw}^{sat}(L)$) is available for Rmims, providing a comparison of data and validation of our experimental. CTAs are inexpensive ammonium surfactants that have antimicrobial properties. For industrial use, CTAs appear most attractive. However, large CTAs (twelve carbon chain and higher) are solids at ambient conditions. BAMs are large compounds that remain in the liquid state at ambient conditions. Although [N6662][Tf_2N] and [Bu(3)MeN][Tf_2N] are not branched RTILs, they resemble the overall BAM class in their bulky nature. Nevertheless, each class has potential as a delivery agent by meeting the aforementioned criterion – namely, water immiscible and water stable at ambient temperatures [4].

EXPERIMENTAL

Synthesis of RTIL via Shake Flask Method

By specifying a desired quantity of RTIL to produce, stoichiometric amounts of reagents to produce the desired RTIL can be calculated. All RTILs for these experiments have a quaternary ammonium or imidazolium cation combined with the bis(trifluoromethanesulfonyl)imide (Tf_2N) anion. RTILs are formed via a precipitation reaction

$$R\text{-}X + Li\text{-}Tf_2N \rightarrow R\text{-}Tf_2N + Li\text{-}X \qquad (1)$$

where R represents the cation species.

To prepare reagents, we solvate each reagent with enough ultrapure water until the reagents dissolves into solution. Then, the two species are mixed together in a vial and vigorously shaken to ensure maximum conversion to the RTIL precipitate. To ensure a complete phase separation, we allow the precipitate to settle for 24 hours and decant the aqueous salt (Li-X) solution. Five rinses and decants are performed to ensure little aqueous salt remains; on the fifth rinse, a water sample is taken for TOC/TN testing. To purify the RTIL, all volatile components are evaporated via a Rotovac, leaving a presumably dry RTIL. For solid ILs, the cake is dried via vacuum oven – only used for [N(16)111][Tf_2N] at a drying temperature of 320 K for three hours .

Total Organic Carbon (TOC)/Total Nitrogen (TN) testing

After allowing an RTIL (less than 1 mL) in contact with ultrapure water to reach equilibrium, a water sample is taken. Based on expected values, stock solutions (KNO_3 for nitrogen, Potassium Hydrogen Phthalate (KHP) for organic carbon) for a calibration curve fit are used. In conjunction, acid water (one drop of phosphoric acid per 100mL-water) is used to ensure a clean line between samples. Using the TOC/TN Analyzer, test the water solution for total organic carbon and nitrogen in the water phase. The analyzer measures the saturated concentration of RTIL in the water phase expressed in ppm; Appendix 1 shows calculations to convert from ppm (µg/L) to $C_{i,w}^{sat}(L)$ (mol/L). The accuracy for testing is as follows: TOC: ±4µg/L, TN: ±5µg/L.

Testing surface tension

We use the Du Nouy ring method via tensiometer for critical micelle concentration (CMC) tests for [N(16)111][Tf_2N] and [N6662][Tf_2N]. Due to possible residual surfactant on the surface of the vessel, clean the 20 mL small vessel and stir bar with acetone, ethanol, and ultrapure water. There are two phases in this system, the vessel and syringe phases. 10 mL of ultrapure water is used in the vessel phase (usually surfactant) and 10 mL of water saturated with RTIL in the syringe phase (usually diluting agent). To ensure any residual chemical species is not in the syringe line, a small fraction is injected to flush the line. Additionally, the Du Nouy ring is cleaned via Bunsen Burner flame. With all necessary data (density, molecular weight, and initial concentration), the CMC analysis is performed by diluting the vessel phase in set volume increments and graphing the associated surface tension versus concentration of the fluid in the vessel. Appendix 3

displays the software inputs. From the data generated figure, draw a baseline horizontal to the plateau and a tangent line from the linear region near the plateau to obtain the CMC.

RESULTS AND DISCUSSION

Table 1 displays data from TOC/TN testing in each RTIL-water equilibrium sample and the calculated $C_{iw}^{sat}(L)$. Although we obtained TOC and TN data, we only used TOC data to progress further in the discussion. By available Rmim literature data, Table 2 shows an order-of-magnitude difference between measured TN and literature values, providing a validation for TOC data versus TN data. We believe the TN values are inaccurate due to the large TN calibration range necessary for obtaining ppm-Nitrogen values. Appendix 1 shows sample calculations to convert the associated ppm-Carbon and ppm-Nitrogen values to a more practical value ($C_{iw}^{sat}(L)$), a solubility measure, to fit our LFER model. Using the LFER empirical model, Figure 1 shows increasing molar volume of the RTIL yields less partitioning to the water phase in a linear fashion. Appendix 2 shows sample calculations of molar volume. From Figure 1, we note deviations from the predicted linear trend; [N6662][Tf_2N] and [N(16)111][Tf_2N] "spike" in solubility, and [N(12)111][Tf_2N] and [N(14)111][Tf_2N] display a horizontal trend. We will discuss these deviations throughout the remainder of this thesis.

Table 1: TOC/TN Data for Calculating $C_{iw}^{sat}(L)$				TOC Data			TN Data		
Compound	**Class**	**Molecular Weight (g/mol)**	**Molar Volume (mL/mol)**	**ppm-Carbon**	**$C_{RTIL,W}^{sat}(L)$ (mol-RTIL/L)**	**$\log C_{RTIL,W}^{sat}(L)$ (mol/mL)**	**ppm-Nitrogen**	**$C_{RTIL,W}^{sat}(L)$ (mol-RTIL/L)**	**$\log C_{RTIL,W}^{sat}(L)$ (mol/mL)**
[C(4)Me$_2$(iPr)N][Tf$_2$N]	BAM	402.3	263.5	1964	1.49E-02	-4.83	332.5	1.19E-02	-4.93
[C(6)Me$_2$(iPr)N][Tf$_2$N]	BAM	426.3	291.7	657.6	4.21E-03	-5.38	124.7	4.45E-03	-5.35
[Bu(3)MeN][Tf$_2$N]	BAM	450.3	319.8	273.2	1.52E-03	-5.82	41.5	1.48E-03	-5.83
[C(10)Me$_2$(iPr)N][Tf$_2$N]	BAM	474.3	348.0	151.5	7.42E-04	-6.13	42.5	1.52E-03	-5.82
[N6662][Tf$_2$N] avg	BAM	578.8	418.5	540.2	2.04E-03	-5.69	83.1	2.96E-03	-5.53
[N(4)111][Tf$_2$N]	CTA	396.4	235.3	1637	1.51E-02	-4.82	7210	2.57E-01	-3.59
[N(6)111][Tf$_2$N]	CTA	424.4	263.5	1117	8.45E-03	-5.07	3042	1.09E-01	-3.96
[N(8)111][Tf$_2$N]	CTA	452.5	291.7	404.1	2.59E-03	-5.59	1130	4.03E-02	-4.39
[N(10)111][Tf$_2$N]	CTA	480.5	319.8	131.7	7.31E-04	-6.14	367.9	1.31E-02	-4.88
[N(12)111][Tf$_2$N]	CTA	516.6	348.0	21.1	1.04E-04	-6.98	2.7	9.51E-05	-7.02
[N(14)111][Tf$_2$N]	CTA	540.7	376.2	23.4	1.02E-04	-6.99	2.3	8.15E-05	-7.09
[N(16)111][Tf$_2$N]	CTA	564.7	404.4	281.7	1.12E-03[A]	-5.95	18.8	6.69E-04	-6.17
[BMIM][Tf$_2$N]	RMIM	419.4	253.0	1457	1.21E-02	-4.92	4838	1.15E-01	-3.94
[HMIM][Tf$_2$N]	RMIM	447.4	281.2	808.5	5.61E-03	-5.25	2022	4.81E-02	-4.32
[C(10)MIM][Tf$_2$N]	RMIM	503.5	337.6	93.7	4.88E-04	-6.31	25.4	6.04E-04	-6.22

A – represents the $logC_{iw}^{sat}(L)$ not accounting for the CMC. The logC_{iw}^{sat} value for [N(16)111][Tf$_2$N] at the CMC is -6.90.

Table 2: Comparison of Experimental Data to Literature				
Compound	C_{iw}^{sat}TOC Data (M)	C_{iw}^{sat} TN Data (M)	C_{iw}^{sat} Literature (M)	Percent Difference
[BMIM][Tf$_2$N]	0.012	0.115	0.017 [6] 0.018 [7]	33%
[HMIM][Tf$_2$N]	0.00561	0.0481	0.00531 [7]	5.60%

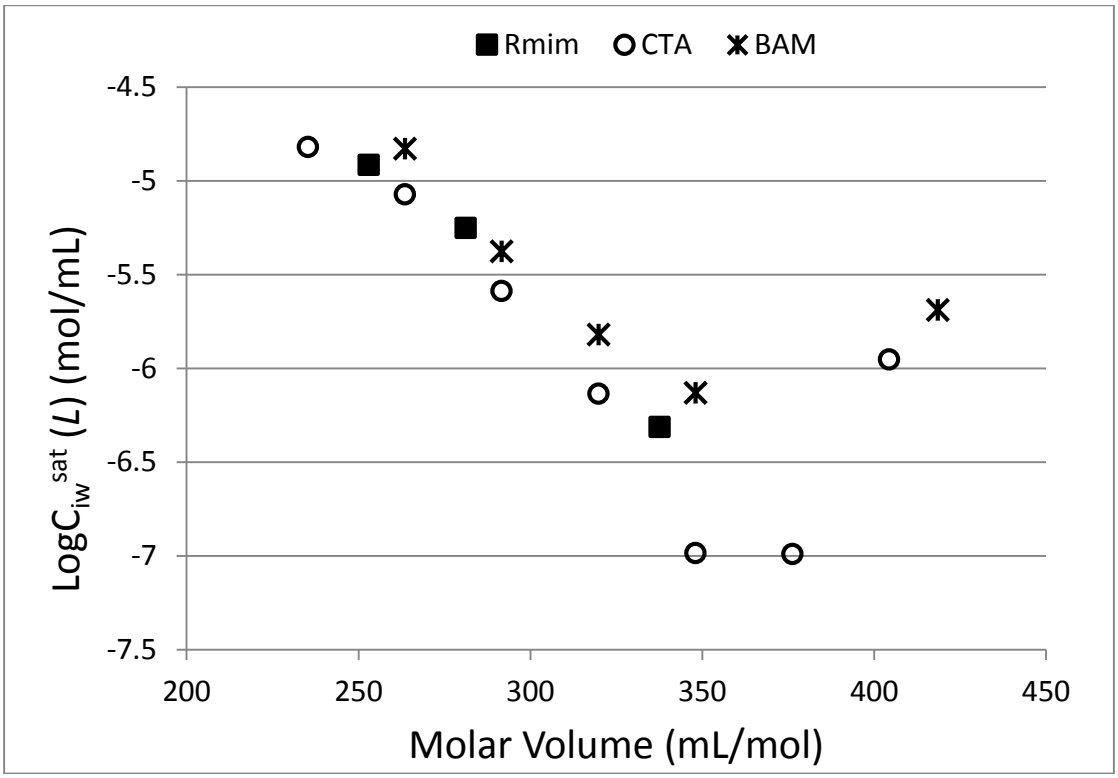

Figure 1: Saturated concentration of RTIL in water as a function of molar volume for 3 classes of RTIL

Figures 2, 3, and 4 represent the empirical model following the form: $logC_{iw}^{sat}(L) = -a(V_{ix}) + b$, for the liquid RTIL. However, Figure 5 shows [N(12)111][Tf_2N] to [N(16)111][Tf_2N] of the CTA class do not obey this observed trend, for these compounds are in a solid phase. The observed trend is a horizontal line; however, [N(16)111][Tf_2N] does not follow the trend. Micellization theory explains this phenomenon, considering the compounds contain a large, hydrophobic alkyl group.

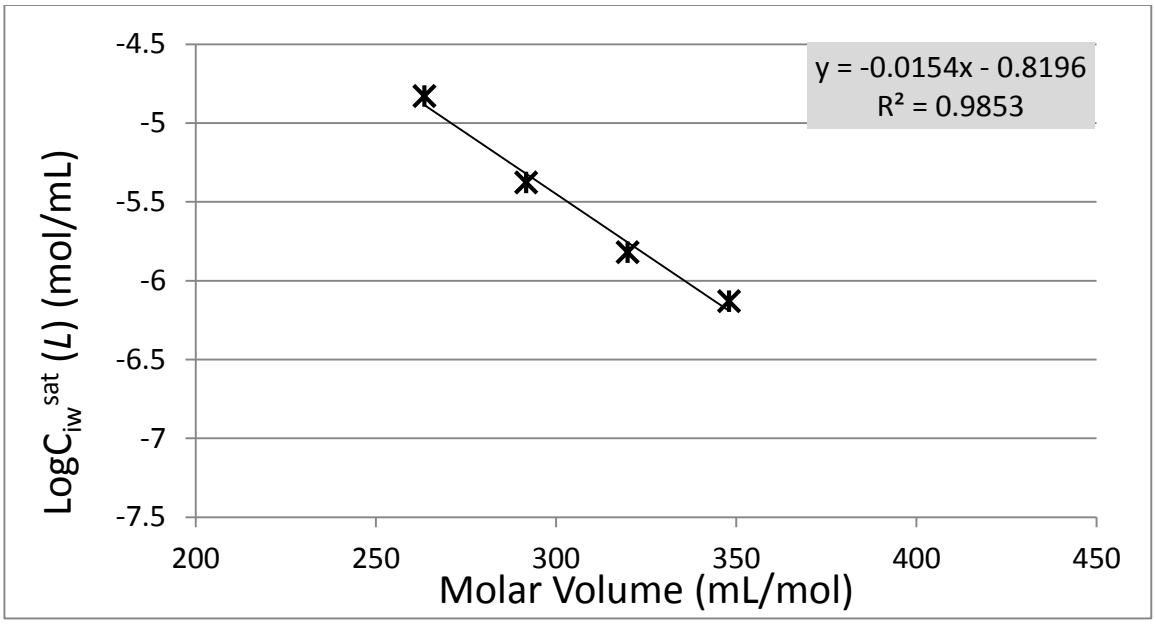

Figure 2: Saturated concentration of BAM[Tf_2N] in water excluding [N6662][Tf_2N].

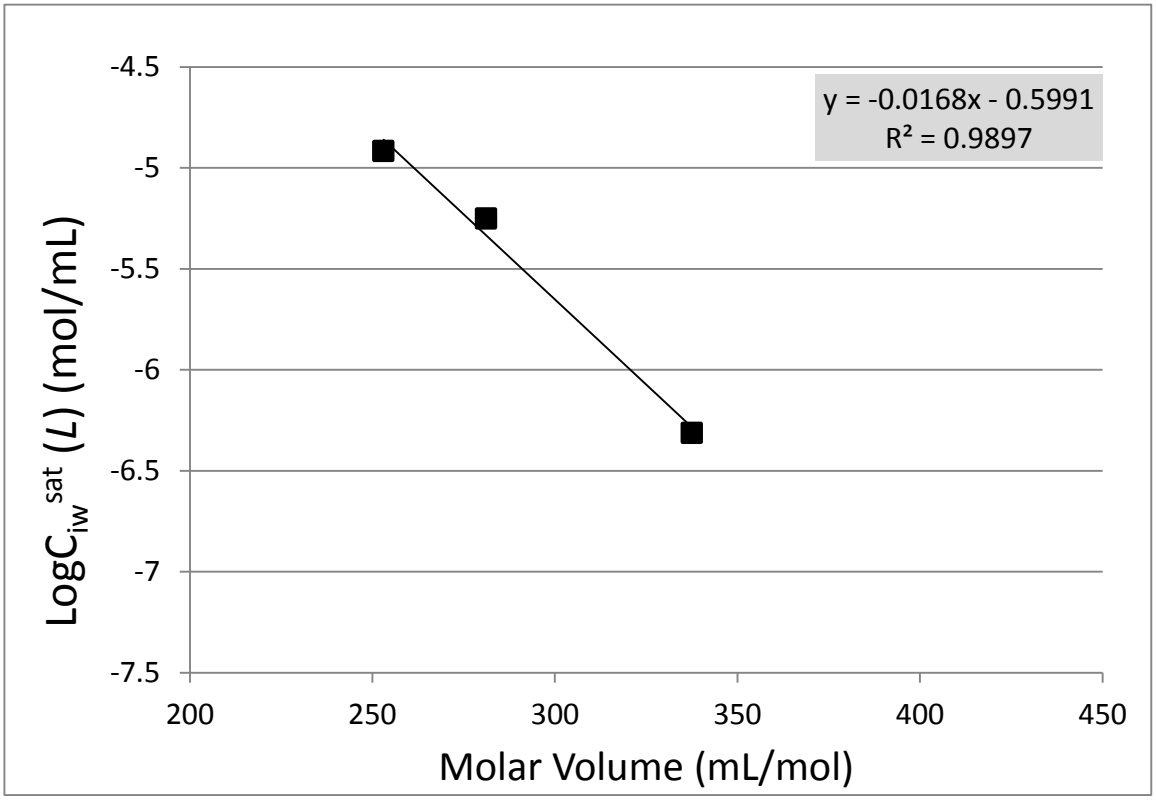

Figure 3: Saturated concentration of Rmim[Tf_2N] in water

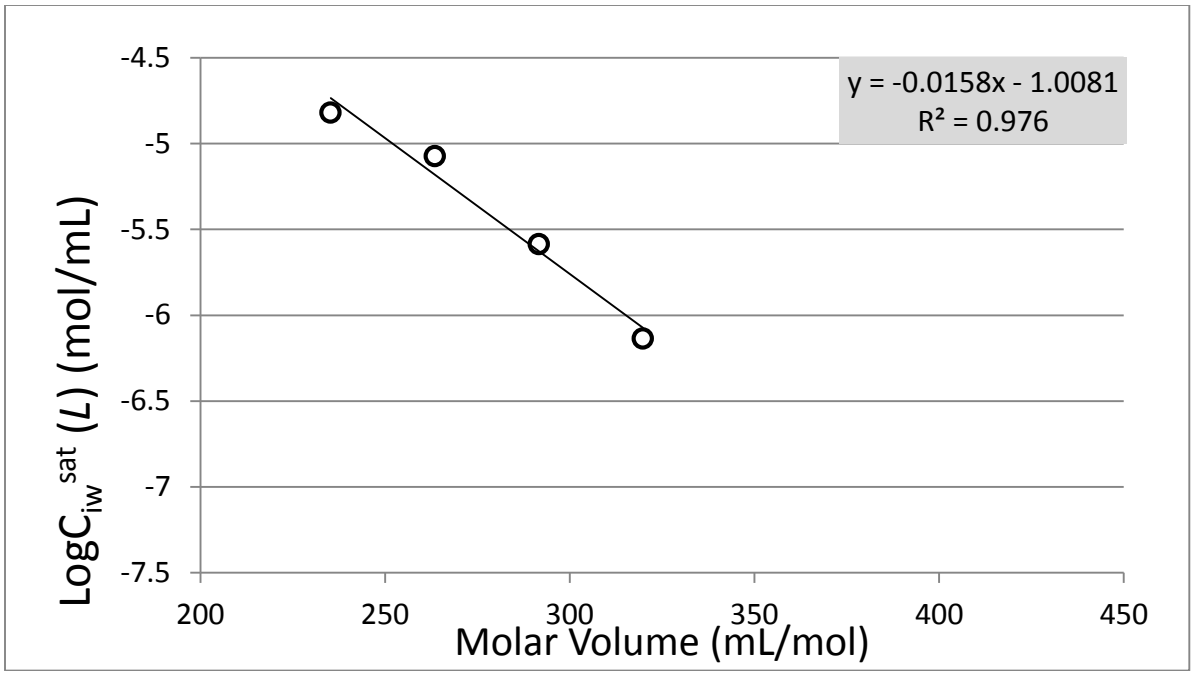

Figure 4: Saturated concentration of CTA[Tf_2N] liquid range, [N(4)111] to [N(10)111].

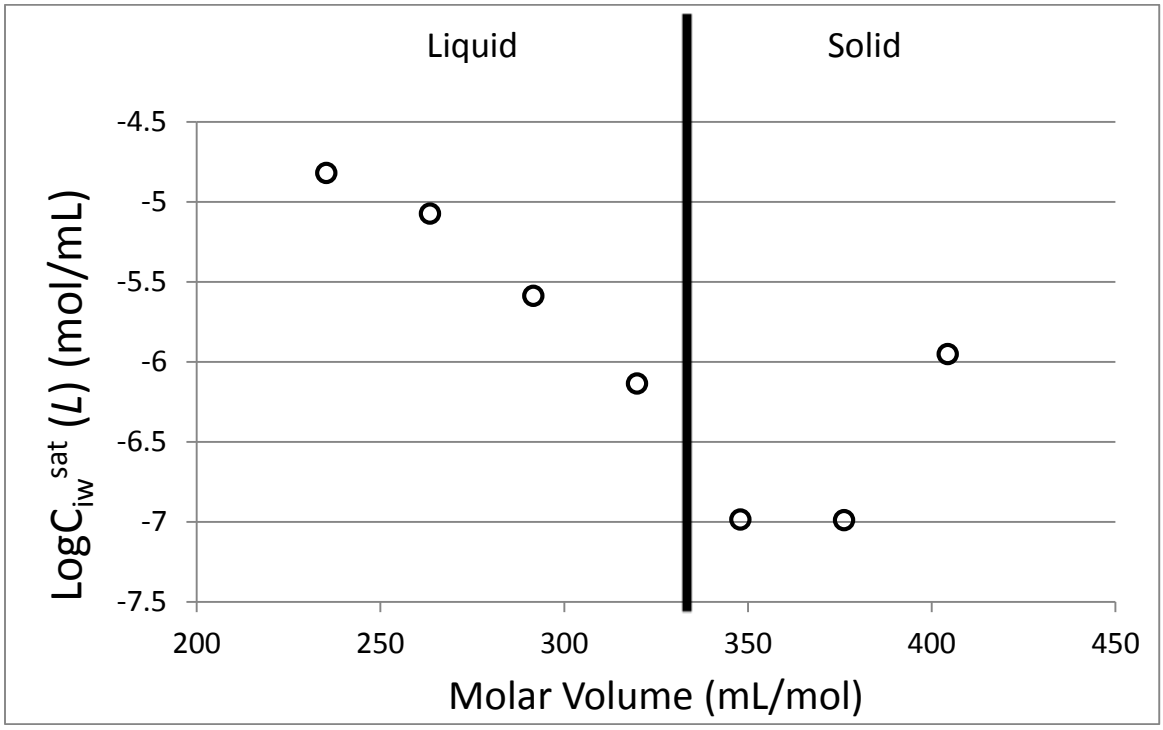

Figure 5: Saturated concentration of CTA[Tf_2N] in water, [N(4)111] to [N(16)111].
Figure 4 displays the linear regression of the liquid range.

To verify the existence of a CMC, we tested for the CMC of [N(16)111][Tf_2N] via tensiometer. In this case, we performed the reverse of the standard procedure by using ultrapure water in the small vessel and adding water saturated with IL (surfactant phase). Figure 6 shows the CMC of [N(16)111][Tf_2N] in water is 12.7 mmol/L, resulting in a corresponding $\log C_{iw}^{sat}(L)$ (mol/mL) of -6.90. This places [N(16)111][Tf_2N] on a horizontal line with the remaining solids, shown in Figure 7.

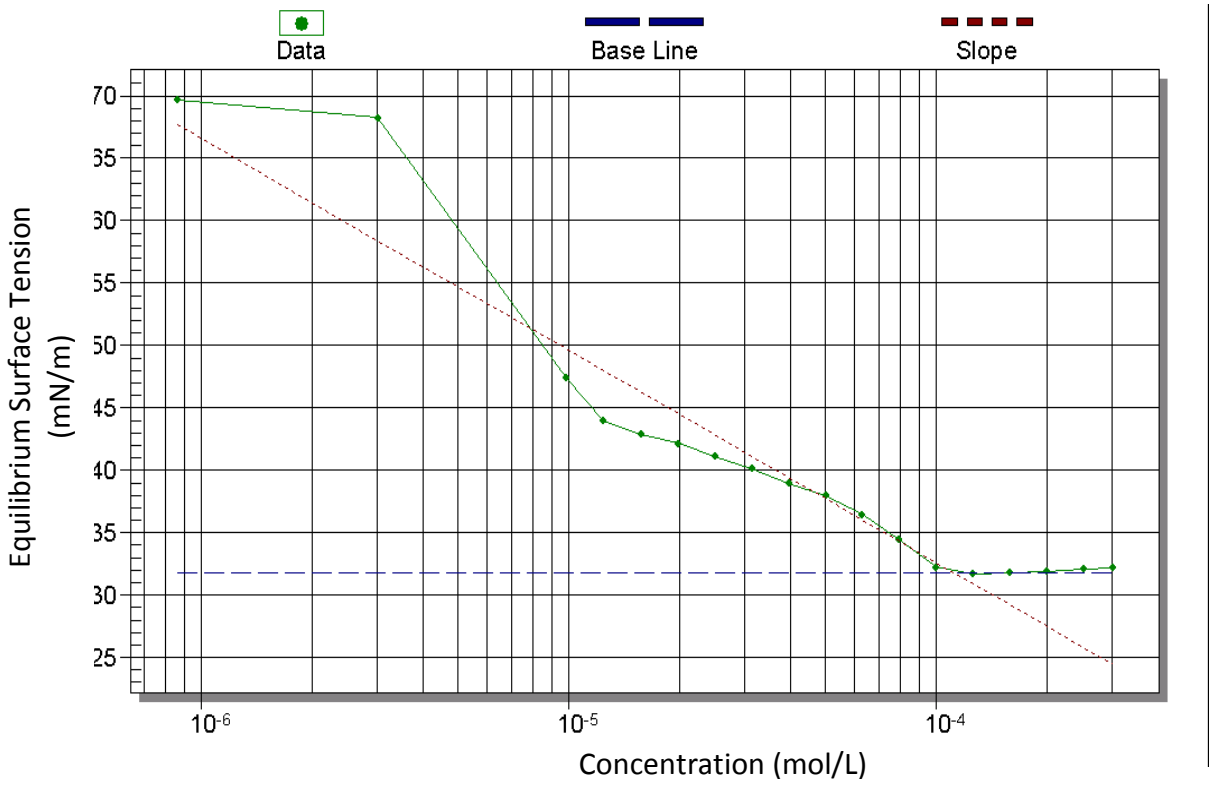

Figure 6: Equilibrium surface tension versus concentration of [N(16)111][Tf_2N] in water to determine CMC.

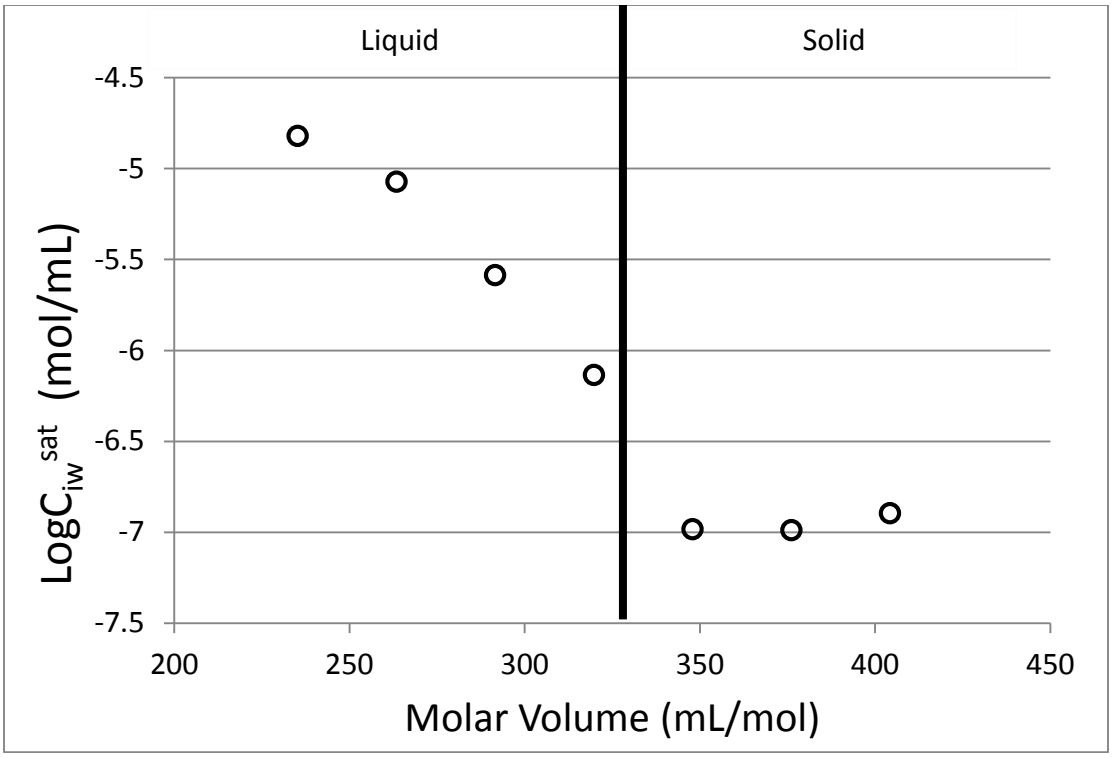

Figure 7: Saturated Concentration of CTA[Tf_2N] corrected for CMC of [N(16)111][Tf_2N]

[N(12)111][Tf_2N] appears to be an IL that deviates from the predicted liquid trend. However, one must consider the nature of the plot and the chemical species involved. Since [N(12)111][Tf_2N] is a solid at room temperature, the $C_{iw}^{sat}(L)$ requires an adjustment to account for its solid state – the low vapor pressure of RTILs makes air partitioning negligible. This adjustment is the ratio of the compound's subcooled liquid fugacity to its natural, solid state fugacity

$$\ln\left(P_{iS}^{*}/P_{iL}^{*}\right) = -[6.8 + 1.2(n-5)]\left[T_m/T\right] \qquad (2)$$

where n is the number of rotational bonds, T_m is the melting temperature of the compound and T is the temperature at which experiments are performed (298 K) [5].

The adjusted $C_{iw}^{sat}(L)$ is of the form

$$C_{iw}^{sat}{}_{L} = C_{iw}^{sat}{}_{S}\left(P_{iL}^{*}/P_{iS}^{*}\right) \quad (3)$$

where subscripts L and S represent the liquid phase and solid phases respectively. As a reference for the validity of this approach, the trend for the liquid CTA region shown in Figure 5 allows us to project the necessary $\log C_{iw}^{sat}(L)$ based on the molar volume, shown in Table 3.

Table 3: Adjusting C_{iw}^{sat} for Solid Compound to Subcooled Liquid

Compound [Tf_2N] Anion	Molar Volume (mL/mol)	Flexible Bonds	T_m (K)	P_{iS}^{*}/P_{iL}^{*}	$C_{iw}^{sat}(L)$ (mol/L)	$\log C_{iw}^{sat}(L)$ (mol/mL)	Model	Percent Difference
[N(12)111]	348.0	19	311	0.36	2.90E-04	-6.54	-6.52	0.28%
[N(14)111]	376.2	21	318	0.17	5.86E-04	-6.23	-6.97	10.5%

As seen in Table 3, the projected and adjusted $logC_{iw}^{sat}(L)$ values are roughly the same for [N(12)111][Tf_2N]. By this logic, [N(12)111][Tf_2N] fits the expected trend with a vapor pressure adjustment, and we conclude that micellization does not apply for [N(12)111][Tf_2N]. However, as seen in Table 3 for [N(14)111][Tf_2N], the percent difference is more dramatic and the adjustment alone cannot be applied due to suspected micellization. Figure 8 provides the LFER model applied including [N(12)111][Tf_2N].

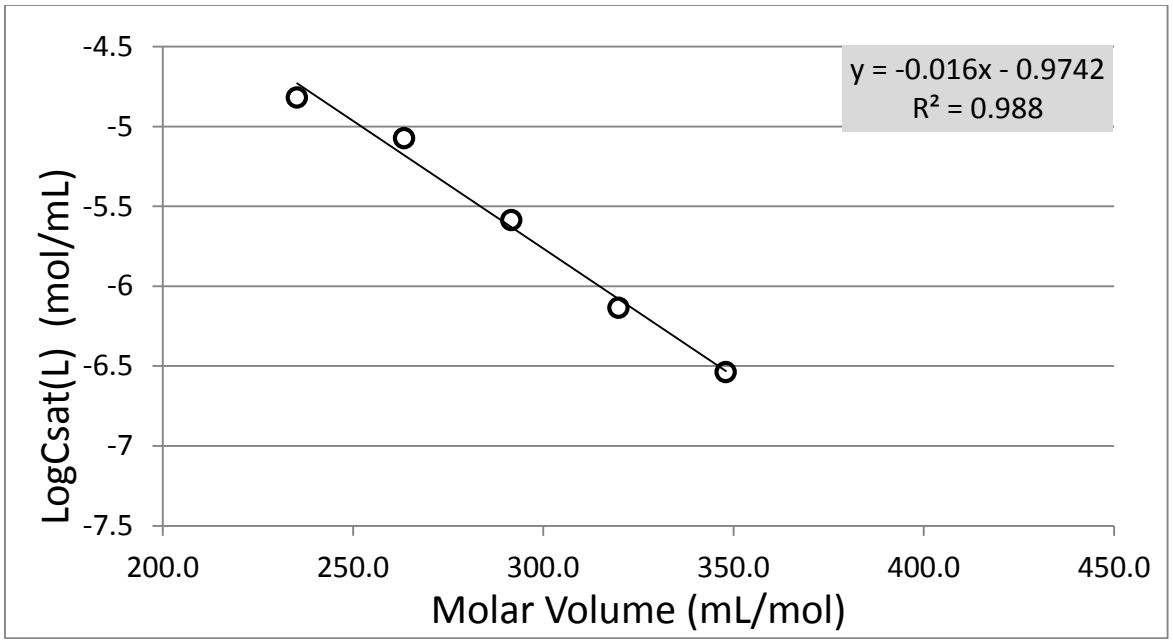

Figure 8: Saturated concentration of CTA[Tf_2N] adjustment for [N(12)111][Tf_2N] [N(4)111][Tf_2N] to [N(12)111][Tf_2N]

[N6662][Tf_2N] also diverges from the linear trend in the BAM class. Figure 9 shows a CMC test using the same reverse process used for [N(16)111][Tf_2N]. The corresponding CMC is not 100% definite due to multiple dilutions – staggers in the figure; however, a CMC does exist. As a hypothesis, the compound will be horizontal to [Bu_3MeN][Tf_2N] as in the case of [N(16)111][Tf_2N]; nevertheless, further experiments are needed to validate the statement.

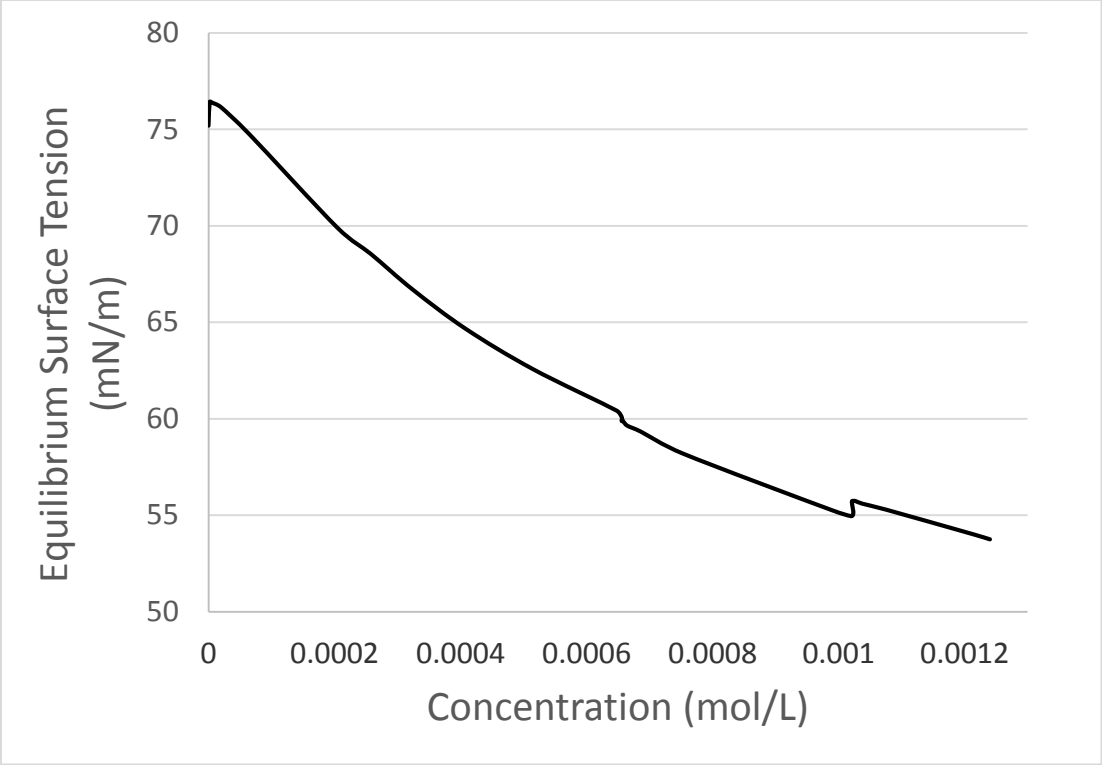

Figure 9: Equilibrium surface tension versus concentration of [N6662][Tf_2N] in water to determine the existence of a CMC.

Considering the optimal RTIL must have a high carrying capacity, low water solubility and remain in the liquid state, the following three RTILs are proposed: [N(10)111][Tf_2N], [N(10)Me_2(iPr)][Tf_2N], and [C(6)MIM][Tf_2N]. The purpose of this research is to obtain preliminary water solubility data for selection of the best RTIL for estimating the partitioning coefficient of the signal (cis-2-decenoic acid) between a water and RTIL phase. Since there was an excess of [N(10)111][Tf_2N] available, it is used to estimate the partitioning coefficient of the signal between an RTIL and water. Since the actual signal (cis-2-decenoic acid) is expensive, we used the saturated version (decanoic acid). Decanoic acid is less polar than cis-2-decenoic acid; the saturated bond of cis-2-decenoic

acid decreases the solubility of the compound. Therefore, there will be some discrepancy between the partitioning coefficients of cis-2-decenoic acid and decanoic acid. As a preliminary step, we developed a model to approximate the expected TOC reading of decanoic acid in the water phase based on the MSDS K_{iow}, where o (octanol) will represent the RTIL. Appendix 3 contains the derivation of the model.

Experimentally, we utilized the shake flask method to determine the partitioning coefficient. In using this method, there are limitations. The $C_{iw}^{sat}(L)$ for decanoic acid prevents large quantities to be introduced into the system. Our system is in a 40 mL vessel, and we introduce 0.5 mL-RTIL to be in contact with a water phase; 0.5 mL-RTIL is used to allow enough signal to remain in the water phase for testing TOC/TN. The volume of RTIL used in this system is not able to carry above 200 mg of signal– at which the RTIL appears to be in a pseudo-solid state. In reaching this point, we used heat and centrifugation to settle suspended particles to force equilibrium. As the concentration of signal in water increases, with the addition of RTIL to the system, an emulsion forms. To ensure suspended RTIL-signal is not in the water sample for TOC/TN testing, we use centrifugation to settle any suspended particles. For an accurate result, the desired TOC reading of the signal must be significant enough to be differentiated from the RTIL in the water phase

$$(TOC_{Total} = TOC_{signal} + TOC_{RTIL}) \qquad (4)$$

The pH of the system due to the acidic nature of the signal is between 3.5 and 4. Based on the pKa of decanoic acid, the fraction in the ionic form is estimated by

$$\alpha = (1 + 10^{pH-pKa})^{-1} \qquad (5)$$

to adjust the partitioning coefficient at a different pH ($Kiow_{pH}$=Kiow*α) [5]. Considering we are discussing aqueous systems, we must account for the fraction in the ionic form that contributes to solubility among the water and RTIL phases.

CONCLUSION

From experiments, additional LFER empirical relationships relating $logC_{iw}^{sat}(L)$ and size (group contribution molar volume) are as follows

$$\text{BAM: } logC_{iw}^{sat}(L) = -0.0154(V_{ix}) - 0.8196$$
$$\text{Rmim: } logC_{iw}^{sat}(L) = -0.0168(V_{ix}) - 0.5991$$
$$\text{CTA: } logC_{iw}^{sat}(L) = -0.016(V_{ix}) - 0.9742$$

where $logC_{iw}^{sat}$ is expressed in (mol/mL) and V_{ix} is expressed in (mL/mol). Values of $logC_{iw}^{sat}(L)$ are reported in Table 1.

At room temperature, ILs in the solid state show a trend of a horizontal line on a graph of $\log C_{iw}^{sat}(L)$ versus molar volume. However [N(16)111][Tf_2N] violates this trend and exhibits micellization when immersed in water. When we apply the aforementioned empirical relationship to this IL using the CMC, we observe the predicted trend. For the case of [N6662][Tf_2N], a similar deviation exists. Through a similar process, we are not able to conclude an exact CMC due to the multiple dilutions performed. However, we expect similar behavior. These ILs behave as surfactants considering these compounds contain a large, hydrophobic alkyl group.

[N(12)111][Tf_2N] appears to deviate slightly from the predicted liquid trend. Considering the the nature of the plot and the chemical species involved (solid at room temperature), the $C_{iw}^{sat}(L)$ requires an adjustment via vapor pressure to account for its solid state. Using the trend in Figure 5, we modeled an expected $\log C_{iw}^{sat}(L)$ and found little percent difference between the two numbers after adjustment for its solid state. Therefore, we conclude that micellization does not apply for [N(12)111][Tf_2N]. However, as seen in Table 3 for [N(14)111][Tf_2N], the percent difference is more dramatic and the adjustment alone cannot be applied due to suspected micellization.

FUTURE WORK

Future steps include using 50 mg, 100 mg, and 150 mg of the signal and compare to the model. With these points, we can estimate an appropriate partitioning coefficient. Considering the low pH of this system, we can adjust the partitioning coefficient at a pH of 7 by including an alpha term $(1 + 10^{pH-pKa})^{-1}$ to account for the fraction in the ionic form. With this overall knowledge, investigation of [N(10)Me_2(iPr)][Tf_2N] and [HMIM][Tf_2N]'s associated partitioning coefficients can be estimated. Once these are known, steps may be taken to approximate the partitioning coefficient of cis-2-decenoic acid between RTILs and water.

REFERENCES

[1] K. Sauer, A. K. Camper, G. D. Ehrlich, J. W. Costerton and D. G. Davies, "Pseudomonas aeruginosa Displays Multiple Phenotypes during Development as a Biofilm," *Journal of Baceriology,* vol. 184, no. 4, pp. 1140-1154, 2002.

[2] M. Pasmore and et al., "Effects of ultrafiltration membrane surface properties of Pseudomonas aeruginosa biofilm initiation for the purpose of reducing biofouling," *Journal of Membrane Science,* vol. 194, pp. 15-32, 2001.

[3] H. Mizuuchi, V. Jaitely, S. Murdan and A. Florence, "Room temperature ionic liquids and their mixtures: Potential pharmaceutical solvents," *European Journal of Pharmaceutical Sciences,* vol. 33, pp. 326-331, 2002.

[4] G. A. Baker and S. N. Baker, "A Simple Colorimetric Assay of Ionic Liquid Hydrolytic Stability," *Aust. J. Chem,* vol. 58, pp. 174-177, 2005.

[5] R. P. Schwarzenbach, P. M. Gschwend and D. M. Imboden, Enivronmental Organic Chemistry, Hoboken, NJ: John Wiley & Sons, Inc., 2003.

[6] J. Ranke, A. Othman, P. Fan and A. Muller, "Explaining Ionic Liquid Water Solubility in Terms of Cation and Anion Hydrophobicity," *International Journal of Molecular Sciences,* vol. 10, no. 3390, pp. 1271-1289, 2009.

[7] N. V. Shvedene, S. V. Borovskaya, V. V. Sviridov, E. R. Ismailova and I. V. Pletnev, "Measuring the solubilities of ionic liquids in water using ion-selective electrodes," *Analytical and Bioanalytical Chemistry,* vol. 381, pp. 427-430, 2005.

[8] R. Condemarin and P. Scovazzo, "Gas permeabilities, solubilities, diffusivities, and diffusivity correlations for ammonium-based room temperature ionic liquids with comparison to imidazolium and phosphonium RTIL data," *Chemical Engineering Journal,* vol. 147, no. 1, pp. 51-57, 2009.

[9] P. Scovazzo, Interviewee, *Associate Professor of Chemical Engineering.* [Interview]. 9 September 2013.

[10] E. Rilo, J. Pico, S. Garcia-Garabal, L. Varela and O. Cabeza, "Density and surface tension in binary mixtures of CnMIM-BF4 ionic liquids with water and ethanol," *Fluid Phase Equilibria,* vol. 285, pp. 83-89, 2009.

APPENDIX

Appendix 1: Converting ppm-Carbon/ppm-Nitrogen to $C_{i,w}^{sat}$

To find the solubility based on total organic carbon, first we must find the fraction of carbon in the compound (f_C) based on the number of carbons in the compound (C_n) and the total molecular weight of the compound (MW).

$$f_C = \frac{C_n * 12.01(gm/mol)}{MW}$$

Now, we can obtain the solubility by

$$C_{i,w}^{sat}(mg/mL) = \frac{ppm - Carbon}{f_C}$$

For finding the solubility based on total nitrogen, the process is similar

$$f_N = \frac{N_n * 14.01(gm/mol)}{MW}$$

$$C_{i,w}^{sat}(mg/mL) = \frac{ppm - Nitrogen}{f_N}$$

Appendix 2: Molar Volume via Group Contribution

By using characteristic atomic volumes, we are able to account for the intrinsic molecular volume and the bulk structure. In this method, all bonds (single, double, triple) are considered equal. The molar volume (V_{ix}) is estimated by adding the following characteristic atomic volumes given in Table 4.

Table 4: Characteristic Atomic Volumes (mL/mol)							
C	16.35	*N*	14.39	*Cl*	20.95	*S*	22.91
H	8.71	*P*	24.87	*Br*	26.21	*Si*	26.83
O	12.43	*F*	10.48	*I*	34.53	*Bond*	-6.56

For example, benzene's molar volume is

$$V_{ix} = 6(16.35) + 6(8.71) + 12(-6.56) = 71.6\, mL/mol$$

In this study, the molar volume is calculated the following group contribution method. Other researchers may consider using the intrinsic molar volume only.

Table 5: Comparison of size parameters			
Compound	**Intrinsic Molar Volume (mL/mol)** [8]	**Group Contribution Molar Volume (mL/mol)**	**Percent Difference**
[N(4)111][Tf_2N]	289.6	235.3	19%
[N(6)111][Tf_2N]	324.5	263.5	19%
[N(10)111][Tf_2N]	393.2	319.8	19%

As shown in Table 5, as long as one uses a consistent method, the same general trend may be reproduced. Therefore, the use of one size parameter versus the other does not affect the accuracy of our results.

Appendix 3: Tensiometer Software Input

When operating the tensiometer, Table 6 displays the associated inputs for our specific test for [N(16)111][Tf_2N].

Table 6: Tensiometer Inputs					
Probe:					
Name	*Type*	*Ring Radius*	*Wire Radius*	*Wetted Length*	*Method*
Standard Ring	Ring	9.545 mm	0.185 mm	119.946 mm	Ring Method
Vessel:					
Name	Diameter	Max Volume			
Small	46 mm	40 mL			
Phase	Name	Density (g/mL)	Surface Tension (mN/m)	Molecular Weight	Volume
Heavy	Water	1	49.70	18.0	20.0
Light	Air	0.0013	-	-	-
	Name	Concentration (mol/L)	Initial Concentration (mol/L)	Molecular Weight	
Addition:	RTIL/Water	0.001	0	18.0	

Appendix 4: RTIL, Water, Signal System Model

In order to model the partitioning system, a mass balance must be performed. The variables are X (mg-Signal/mL-water), Z (mg-Signal/mL-RTIL), Vw (mL-water), V_{RTIL} (mL-RTIL), and S (mg-Signal).

$$Overall: \quad X(Vw) + Z(V_{RTIL}) = S$$

$$Partitioning: \quad K_{iow} = Z/X$$

$$Combining: \quad X(Vw) + X(K_{iow})V_{RTIL} = S$$

$$Rearrange: \quad X(Vw + K_{iow}V_{RTIL}) = S$$

$$Concentration\ in\ Water\ Phase: \quad X = \frac{S}{Vw + K_{iow}V_{RTIL}}$$

$$Concentration\ in\ RTIL\ Phase: \quad Z = K_{iow}X$$